Journal of ELECTRONIC MATERIALS, Vol. 50, No. 1, 2021
https://doi.org/10.1007/s11664-020-08595-9

ORIGINAL RESEARCH ARTICLE

Influences of Ag and In Alloying on Microstructure and Mechanical Properties of Sn-58Bi Solder

JIE YANG,[1,2] QINGKE ZHANG ,[1,3] and ZHENLUN SONG[1]

1.—Key Laboratory of Marine Materials and Related Technologies, Zhejiang Key Laboratory of Marine Materials and Protective Technologies, Ningbo Institute of Materials Technology and Engineering, Chinese Academy of Sciences, Ningbo 315201, People's Republic of China. 2.—Institute of Metal Research, Chinese Academy of Sciences, Shenyang 110016, People's Republic of China. 3.—e-mail: zhangqingke@nimte.ac.cn

Ag (2.0 wt.%) and In (1.5 wt.%) were alloyed into Sn-58Bi eutectic solder, and the individual and combined influences of Ag and In on the microstructure, microhardness, and impact toughness of the SnBi solder were investigated. The results reveal that the microstructures of the SnBiAg, SnBiIn, and SnBiAgIn alloyed solders are coarser than that of the SnBi eutectic solder. Fine Ag3Sn particles are formed in the SnBiAg and SnBiAgIn solders, while small regions of In-rich phases appear in the SnBiIn and SnBiAgIn solders. The microhardness of the three alloyed solders are higher than the SnBi solder, and the Sn-rich phases in the alloyed solders show higher nanohardness, while the nanohardness of the Bi-rich phases with Ag and In addition changes little. The impact toughness of the SnBiAg, SnBiIn, and SnBiAgIn solders are observed to be higher than the SnBi solder, especially in the case of the SnBiAgIn solder. The improvement in ductility of the Sn-rich phase induced by the In solution, and the strengthening effect from the Ag3Sn particles are predicated to be the reason for the increase in impact toughness. The fracture surfaces demonstrate that plastic deformation of the SnBiAgIn solder during the impact process is more obvious. Overall, the combined addition of Ag and In can increase the microhardness and impact toughness of SnBi eutectic solder.

Key words: SnBi solder, Ag and In addition, microhardness, nano-indentation, impact toughness, fracture mechanism

INTRODUCTION

The low melting point of Sn-58Bi eutectic solder (138.9°C) can avoid thermal damage during the soldering process, making it more suitable for soldering of temperature-sensitive devices or components.[1–3] Moreover, the application of low-temperature solder can significantly reduce energy consumption during the reflow soldering process.[4,5] Additionally, Bi metal is relatively cheap. Therefore, Sn-58Bi solder is considered to be promising in mass applications of low-temperature soldering, such as in the electronic and photovoltaic industries.[6,7] Usually, SnBi solder shows superior ductility at a low strain rate.[8] However, because of the inherent brittlement of Bi metal, there exists a high risk of brittle fracture for Sn-58Bi eutectic solder and its impact toughness is quite pool, so that even a common shock or drop can result in fracturing of SnBi/Cu solder joints. As a sudden impact might be encountered during device assembly, shipping, or thermal shock/cycling,[9] this poor impact resistance prevents the wide application of SnBi eutectic solder.[7] In addition, Bi segregation occurs at long-term-aged SnBi/Cu joint interfaces resulting in an embrittlement.[10,11]

Currently, the solderability and some mechanical properties of SnBi solder have been successfully

(Received August 12, 2020; accepted October 28, 2020; published online November 12, 2020)

improved through the incorporation of a series of alloy elements, such as Ag, Ni, Cu, Co, and In, and some rare earths (RE).[12–17] Among these alloy elements, it has been reported that alloying Ag into SnBi solder can improve creep resistance, strength and wettability,[13,14] and Bi segregation was eliminated at long-term-aged SnBiAg/Cu interfaces.[15] The alloying of Ni can improve the elastic modulus, and the tensile and yield strength of Sn-58Bi solder during solid-state aging,[16] and doping of Cu or Zn into SnBi solder can improve the strength through refining the microstructure.[18] With the addition of the In element, the melting point of Sn-58Bi solder can be decreased and the wettability improved, while the elongation of the SnBi-In solder was also obviously increased, i.e., the solder became more ductile.[19,20] Furthermore, the combined effects of Ag, Cu, In, Zn, and RE on SnBi solder have also been revealed.[18,21–23] SnBi solder containing In and Ag exhibited a good combination of higher creep resistance, good mechanical properties, and lower melting temperatures compared with Pb-Sn eutectic solder.[22] In addition, Bi segregation and aging embrittlement were also eliminated in SnBiAgIn/Cu solder joints.[21] Based on the results, the Ag and In elements can be considered to be effective in the optimization of Sn-58Bi eutectic solder, whereas, thus far, little attention has been paid to the influence of Ag and In on the microhardness and toughness of SnBi eutectic solder. Also, there are still few studies on the development of Sn-Bi series solder with a higher impact toughness.

During the early research processes conducted by the authors, it was found that the anti-dropping capability of SnBiAgIn/Cu solder joints is higher, and it is predicated that the combined addition of Ag and In may also be able to improve the impact toughness of SnBi solder. To further optimize the composition and toughness of SnBi solder, in this study a lower content Ag and In were added into Sn-58Bi eutectic solder alone or in combination, and their influences on the microstructure, microhardness, nanohardness, and impact toughness of Sn-Bi eutectic solder as well as the impact fracture behavior were studied. As the content of Ag (4.0 wt.%) and In (3.0 wt.%) in the previous study was relatively high, bulk large Ag_3Sn intermetallic compound (IMC) plates were formed in the SnBiAg solder and a low-melting point phase was formed in the SnBiIn solder;[21] therefore lower contents of Ag and In were used to better explore the content of Ag and In. It is hoped that this work can be helpful in facilitating further applications of SnBi series solders.

EXPERIMENTAL PROCEDURE

Preparation and Characterization of Solders

The Sn-58Bi (wt.%) eutectic solder used in this study was purchased commercially. The alloyed solders were obtained by adding 2.0 wt.% of Ag and 1.5 wt.% of In separately or in combination into s Sn-58Bi alloy, and are here named SnBiAg, SnBiIn and SnBiAgIn, respectively. The lower contents of Ag and In were chosen to avoid the formation of bulk Ag_3Sn plates and a low-melting-point In-rich phase.[21] It should be noted that the weight percentages of the alloy elements are their percentages in the obtained alloyed solders. The SnBiAg and SnBiAgIn solders were smelted in Al_2O_3 ceramic crucibles at 500°C for 0.5 h with Ar protection, and the SnBiIn solder was smelted at 200°C in air with the protection of flux. After the smelting, all the solders were remelted at 200°C in air and cast into bulks with the size of 20 mm × 10 mm × 100 mm. . Then, the solder bulks were aged at 120°C for 24 h so that their microstructures reached a steady state. The aged solders were embedded in epoxy resin and their surfaces were progressively mechanically ground with SiC abrasive paper to 2000-grit, polished with diamond polishing slurry, and ultrasonically cleaned with deionized water and anhydrous ethanol in turn for 20 min. The microstructures of the solders were observed by a FEI Quanta 250 scanning electron microscope (SEM) under the backscattered electron (BSE) imaging mode, and the element distribution in the SnBiAgIn solder was analyzed by an energy dispersive spectrometer (EDS). The phases in the four solders were characterized by a Bruker Axs D8 Discover x-ray diffraction spectroscopy (XRD).

Microhardness and Nano-indentation Tests

As the impact toughness of the solders were tested using bulk solders, the microhardness and nano-indentation tests were also conducted on the polished surfaces of the bulk solders for comparison. The micro-Vickers hardness tests of the solders were carried out by a Digital Vickers Microhardness tester (HV-1000) at an applied load of 25 g and a dwell time of 15 s. At least five indentations were conducted on each solder to obtain the average value. To characterize the nanohardness and plasticity of the Sn-rich and Bi-rich phases in the solders, nano-indentation of the phases was tested by a nano-indenter (MTS-G200) at surface approach velocity of 10 nm/s, a strain rate target of 0.05 s^{-1}, a depth limit of approximately 300 nm, a peak hold time of 10 s, and a Poisson's ratio of 0.33. A triangular pyramid diamond Berkovich indenter with a half angle of 65.3° was used in the indentation test. Since the size of the indentations is thinner than the eutectic lamina spaces of SnBi-based solders, the indentations can usually be pressed on a single phase and the nanohardness of the phase can be identified. However, the indentations may also locate at the boundary of the Sn-rich phase and the Bi-rich phase, so 18 nano-indentations were performed on each solder to ensure enough indentations could be pressed on a single phase, and the mean nanohardness of the Sn-rich phases and the Bi-rich phases were calculated from

3∼5 nanohardness values. The load–displacement curves of each indentation were recorded. After the tests, all the indentations were observed by SEM.

Impact Tests and Fracture Surfaces Observation

The impact toughness tests were performed with a digital display cantilever impact testing machine, with the specimen was clamped in the middle. The initial angle α was 150° and the maximum impact energy was 2.75 J. The dimension of the impact samples was 20 mm × 3 mm × 2 mm. All the sides of the samples were ground with 2000-grit abrasive paper, and the impact surfaces and side surfaces of the specimens were polished for fracture surface observation. At least three samples were tested for each kind of solder to obtain an average value. The patterns of the fracture surfaces and side surfaces of the cracked specimens were observed by SEM under a secondary electron imaging mode to reveal and compare the fracture behavior.

RESULTS AND DISCUSSION

Microstructure and Phases of Solders

The BSE images of SnBi(AgIn) series bulk solders aged at 120°C for 24 h are shown in Fig. 1. As shown in Fig. 1a and b, the SnBi eutectic alloy is composed of the gray Sn-rich phase (β-Sn) and the white Bi-rich phase, and presents as a fine interlocked alternate-layered structure. With 2.0 wt.% of Ag addition, the microstructure shows a little coarsening (see Fig. 1c and d). The microstructure of the SnBiIn solder is coarser, i.e., the lamellar thickness is much thicker than that of the SnBi and SnBiAg solders, as shown in Fig. 1e and f, whereas the SnBiAgIn solder is similar to the SnBiAg solder and only a little coarser than that of the SnBi solder (see Fig. 1g and h). Among the four solders, the microstructure of the SnBiIn solder is the coarsest and that of the SnBi solder is the finest, because the melting point of SnBiIn is lower and the normalized temperature (T/T_m) is relatively high. As a result, alloying with In alone can lead to much greater influence on Bi coarsening compared to Ag or Ag and In together. For the Ag-containing solders, fine Ag_3Sn particles can be observed in the Sn-rich phase at a higher magnification, as presented in Fig. 1d and h, which is consistent with some previous literature,[13,14] while large plate-like Ag_3Sn grains were not observed. Therefore, it is predicated that a proper content of Ag can form fine Ag_3Sn particles and avoid the formation of large Ag_3Sn plates. In addition, it has been reported that the InBi phase can be formed in SnBiIn solder,[20] while little InBi phase can be observed in the SnBiIn and SnBiAgIn solders in this study.

To reveal the distribution of the Ag and In elements, EDS mapping of the solders were conducted. For the EDS equipment used in this study, an element with an atomic ratio higher than 0.5% is detectable. The detection time was chosen to be about 10 min to better show the In and Ag mapping. Figure 2 presents the element distribution in SnBiAgIn solder as an example. It can be seen that the In distribute mainly in the Sn-rich phase, with no In-rich phase, which further demonstrates that most of the In element has dissolved into the β-Sn phase while the InBi phase can hardly be formed with the current content of In. In contrast, the contents of Ag in both the Sn-rich phase and the Bi-rich phase are very small, because the solubility of Ag in Sn and Bi is very low, and most of the Ag element forms into Ag_3Sn IMC. Therefore, the In element can strengthen the β-Sn phase through solid solution, and the fine Ag_3Sn particles can play the role of precipitation strengthening.

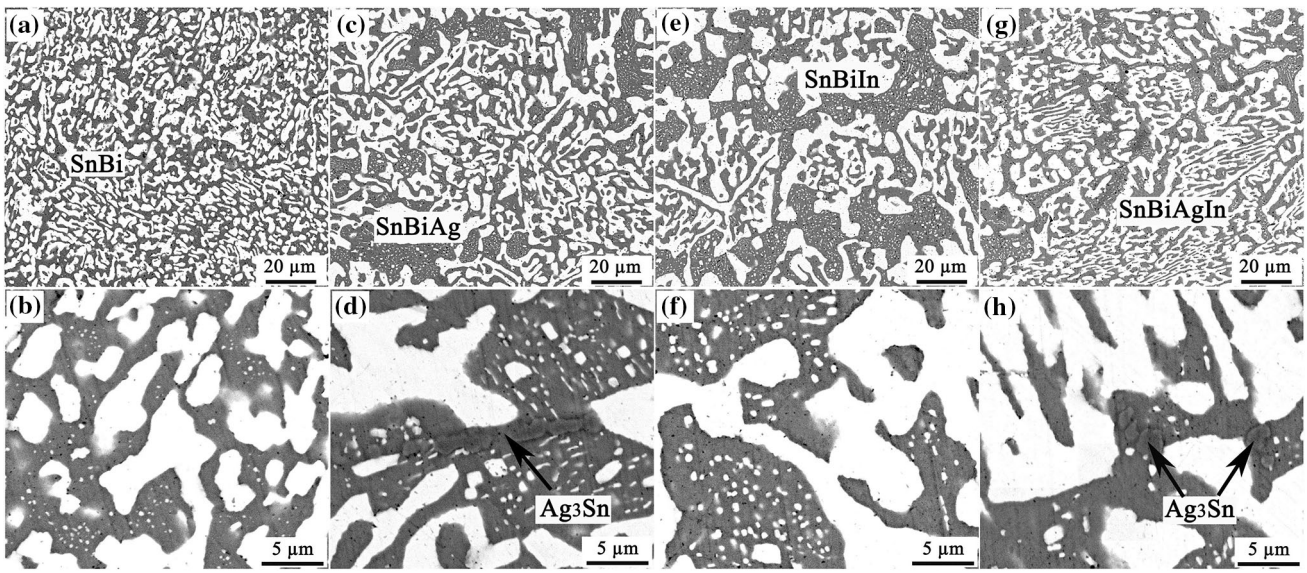

Fig. 1. Microstructures of the bulk solders aged at 120°C for 24 h: (a, b) SnBi, (c, d) SnBiAg, (e, f) SnBiIn and (g, h) SnBiAgIn.

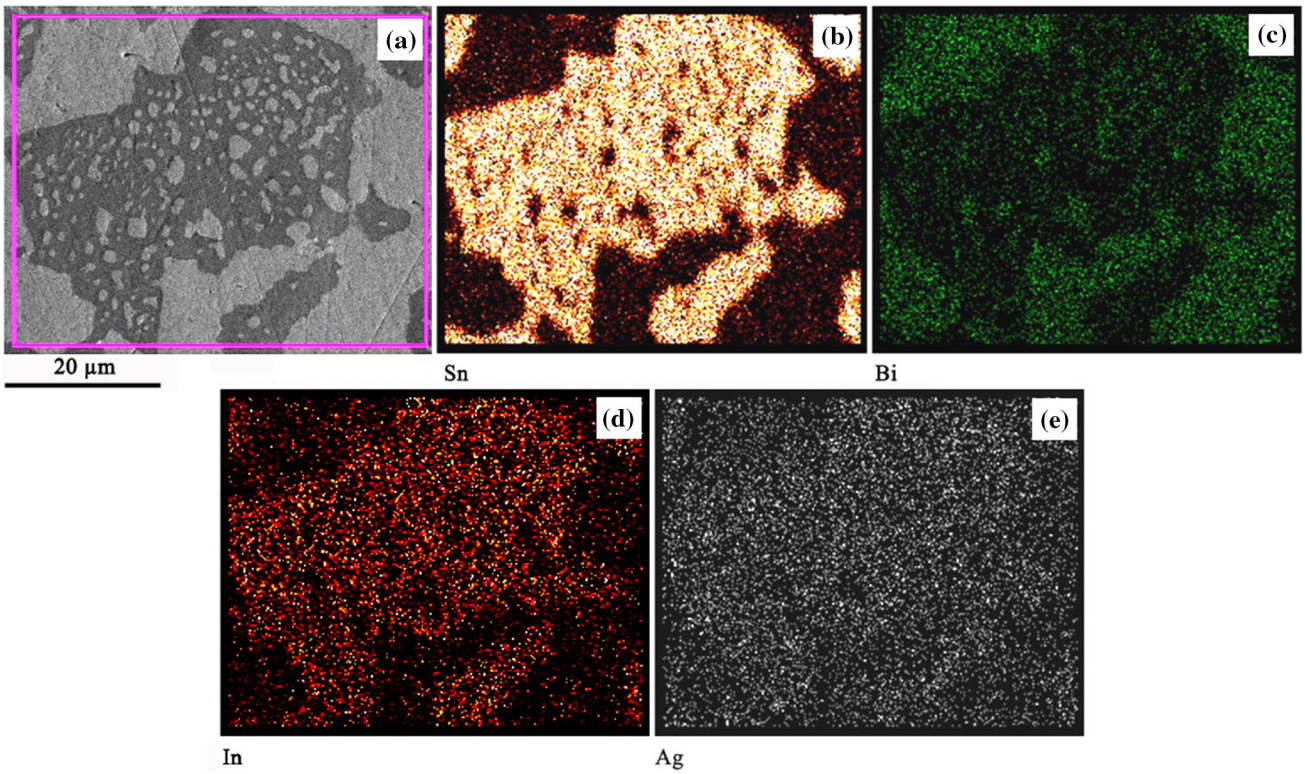

Fig. 2. Element distribution in SnBiAgIn solder: (a) morphology of solder; EDS mapping of (b) Sn, (c) Bi, (d) In, and (e) Ag elements.

To better characterize the phases formed in the alloyed solders, the phases of the four solders were characterized by XRD and the results are presented in Fig. 3, from which it can be seen that the XRD patterns of the four solders are very similar, mainly composed of the β-Sn and Bi-rich phases. With the Ag addition, a small amount of Ag_3Sn IMC can be identified in the BSE images, but its diffraction peaks are quite weak and can be easily covered by the peak of the Bi phase, because the content of Ag_3Sn is small and the Ag_3Sn particles are very fine. For the SnBiIn and SnBiAgIn solders, the InBi and $InSn_{19}$ phases reported in some early publications were not detected, which fits with the SEM images and the EDS mapping results.

Microhardness and Nano-indentation

The microhardness of SnBi(AgIn) series solders are presented in Fig. 4. The average microhardness of SnBi solder is 19.75 $HV_{0.025}$, slightly lower than that of the SnBiIn alloy (21.5 $HV_{0.025}$) and the SnBiAgIn solder (21.99 $HV_{0.025}$), which can be attributed to the solid solution strengthening of In. As the solubility of Ag in Sn is far lower than that of In, and most of the Ag element in the SnBiAg solder forms into the Ag_3Sn IMC, the solid solution strengthening effect of Ag should be less obvious.[24] However, the Ag alloy element can also increase the microhardness of the solder due to the precipitation strengthening effect of the Ag_3Sn particles, making the average microhardness of the SnBiAg alloy (22.1 $HV_{0.025}$) also slightly higher than that of the SnBi solder. As the $AgIn_2$ IMC can be formed between Ag and In,[25] the solid solution strengthening effect of In might be restrained to some extent when Ag and In are added together, and thus the microhardness of the SnBiAgIn alloy is not higher than that of SnBiAg and SnBiIn. To further reveal the effects of the Ag and In elements on the hardness and deformation behavior of the two phases in SnBi solder, nano-indentation tests were conducted on the Sn-rich phases and the Bi-rich phases of the four solders.

Figure 5 shows the nanohardness of the Sn-rich phases and the Bi-rich phases in the four different solders. The nano-sized indentations were pressed into the solders as arrays, and only the nanohardnesses of the indentations fully pressed into a single phase were calculated. Although the Bi-rich phase is usually considered to be hard and brittle, the nano-indentation results reveal that the nanohardnesses of the Sn-rich phases in SnBi(AgIn) series solders are higher than those of the Bi-rich phases. The Sn-rich phases in the three alloyed solders increased obviously compared with those of SnBi solder, which fits with the microhardness of the solders. Moreover, the nanohardness of the Bi-rich phase is basically unchanged. According to the phase diagrams and the EDS mapping results, the Ag and In elements have very low solubility in the Bi-rich phase, and thus the nanohardness of the Bi-rich phase is hardly affected by the alloy elements.

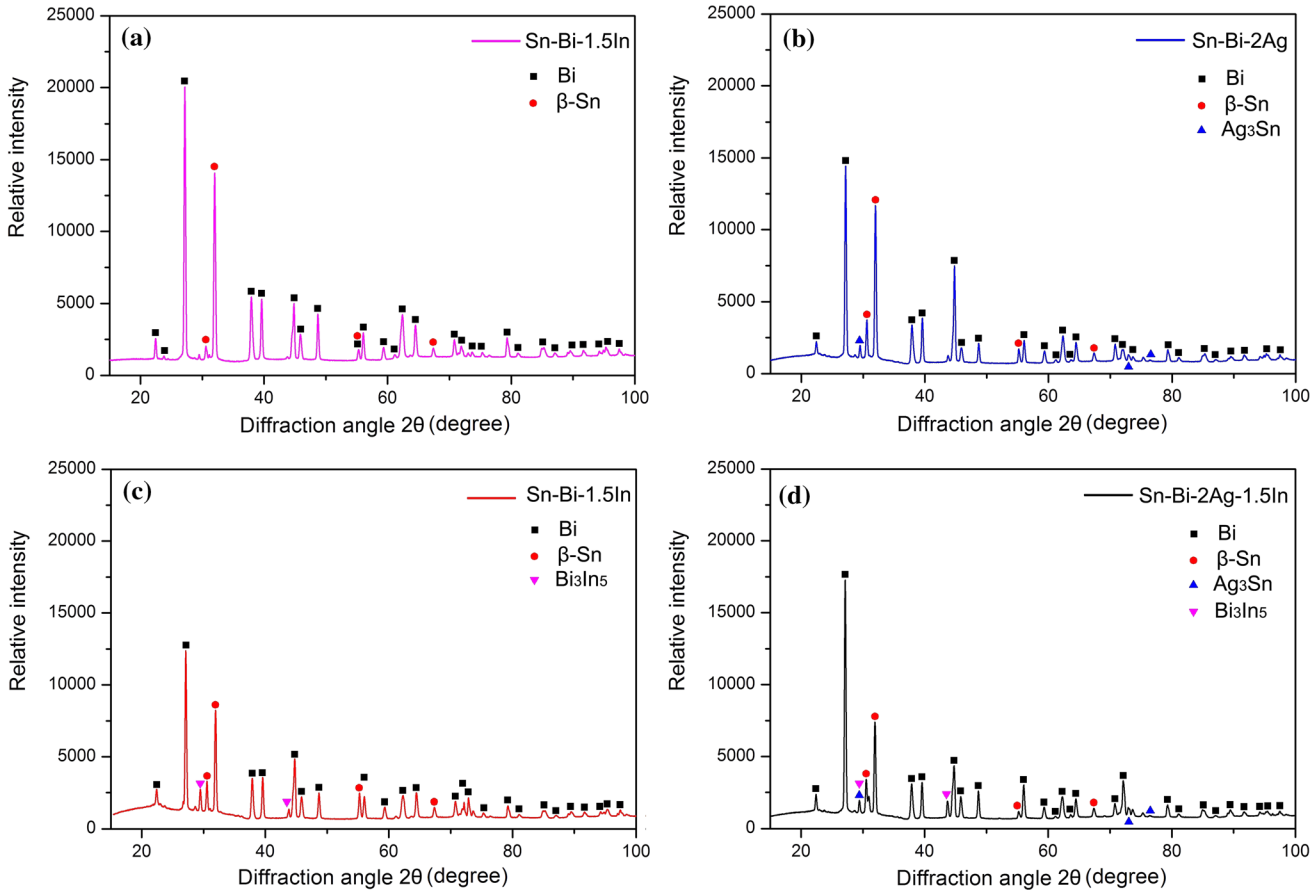

Fig. 3. Surface XRD patterns of the (a) SnBi, (b) SnBiAg, (c) SnBiIn, and (d) SnBiAgIn solders.

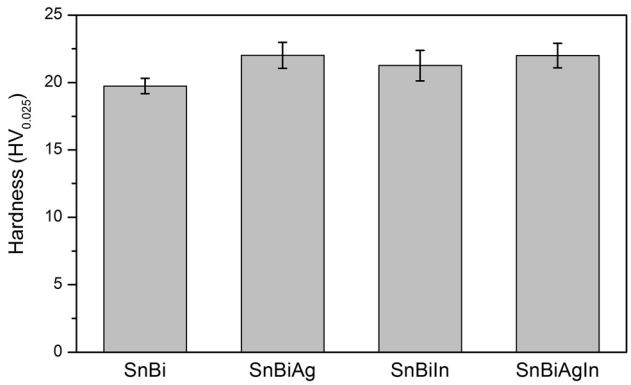

Fig. 4. Microhardness of SnBi, SnBiAg, SnBiIn, and SnBiAgIn bulk solders under a load of 25 gf.

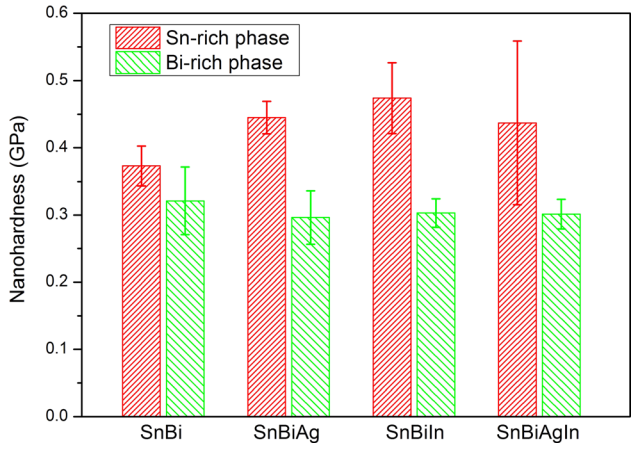

Fig. 5. Nanohardness of the Sn-rich phases and the Bi-rich phases in the bulk SnBi, SnBiAg, SnBiIn, and SnBiAgIn solders.

Figure 6 presents the nanohardness–depth curves and the corresponding indentations of the two phases in the four different solders. As seen in the figure, at the same indentation depth, the load on the Sn-rich phases is always higher than that on the Bi-rich phases. When the indentation depths reach the maximum, the applied loadings on the Sn-rich phases are also higher than those on the Bi-rich phases. Among the Sn-rich phases, their indentation curves in the SnBi and SnBiAg solders are close, and their curves in the SnBiIn and SnBiAgIn solders are also close, while the curves of the two groups are different, as in Fig. 6a. As the solubility of Ag in the Sn-rich phase is much lower than that of In, the Ag element alloy shows less influence on the deformation property of the Sn-rich phase if the Ag_3Sn is not considered. As a result, the nano-indentation curve of Sn-rich phase in SnBiAg solder is similar to that in SnBi solder. For the Bi-rich

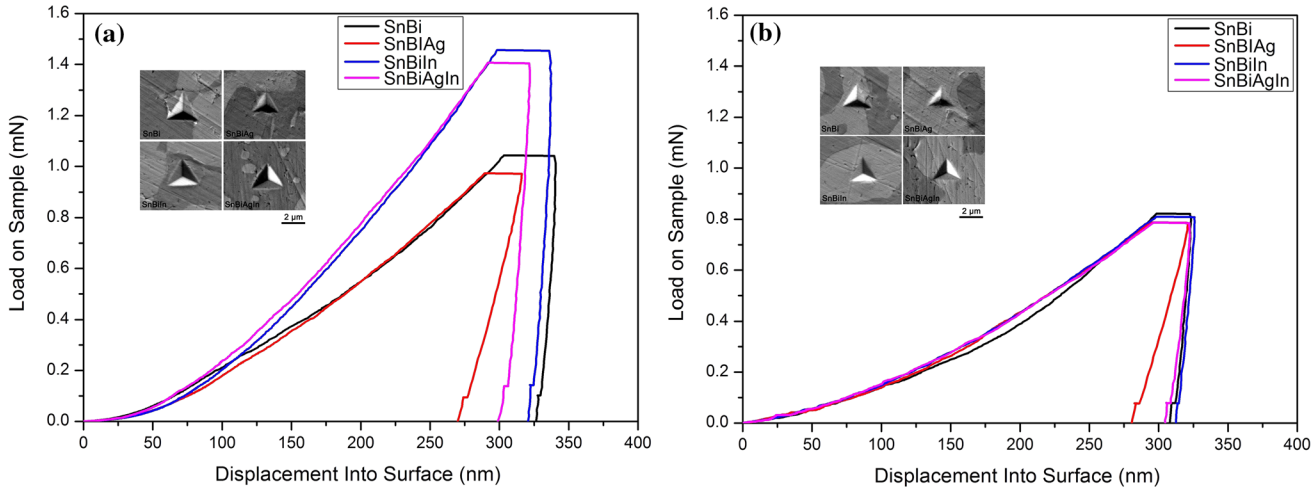

Fig. 6. The load on the sample versus displacement into the surface of the (a) Sn-rich phases and (b) Bi-rich phases of the bulk solders; *insets* show the indentations.

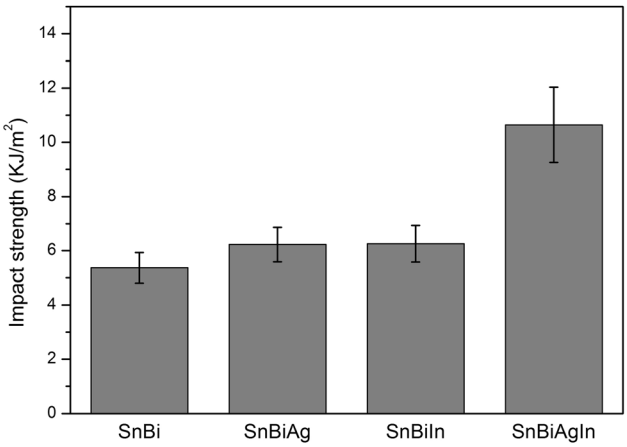

Fig. 7. Impact strengths energy of the four bulk solders.

phases, the nano-indentation curves are similar for all the solders, as exhibited in Fig. 6b, because the Ag and In have little solubility in Bi. Morphologies of all the indentations on different phases corresponding to the curves were inserted in the images. As the indentation depth is the same, the size of the indentations are similar except that in SnBiAg solder, probably because the residual plastic deformation of the two phases in SnBiAg solder is lower and the size of the indentations are smaller.

Impact Toughness and Fracture Behavior

The impact toughness (impact strength) can be expressed by the value of the impact energy, which is presented in Fig. 7. It can be seen that the average impact energy of the SnBi eutectic solder is the lowest, only 5.37 kJ/m^2. The lowest impact energy indicates that the SnBi eutectic solder is the most brittle. The impact energy of the SnBiAg and SnBiIn solders are a little higher than that of the SnBi solder, but not obviously. Although the nanohardness of the Sn-rich phases in the two solders clearly increased, the greater hardness usually corresponds to lower impact toughness, whereas the impact energy of the SnBiAgIn increases significantly to about 10.5 kJ/m^2. In other words, the impact energy was obviously improved by adding a small amount of Ag and In elements in combination. However, when the two alloy elements are added separately, the impact toughness was only increased a little.

In order to further reveal the impact fracture mechanisms of the solders, the fracture surfaces and side surfaces of the SnBi and SnBiAgIn solders were observed for comparison, as shown in Fig. 8. For the impact surfaces, it can be seen that there are some microcracks in the SnBi solder (see Fig. 8a), which were formed during the impact process, because the solder is quite brittle. From the side view, the side surface of the SnBi solder is vertical to the impact direction, i.e., plastic deformation of the solder is very small, as presented in Fig. 8b. From Fig. 8c, it can be seen that the impact fracture surface of the SnBi solder is similar to the tensile fracture surface,[8,21] and that the cleavage fracture is the major fracture mode. For the SnBiAgIn solder, however, few microcracks can be seen on the impact surface, as shown in Fig. 8d. Also, an obvious bending of the solder can be found from the side view, and the plastic deformation characteristics of the solder at the impact side can be seen (see Fig. 8e), which confirms that the SnBiAgIn solder has a higher ductility and toughness, which is consistent with the results of the impact surface and impact strength. However, the difference in the fracture surfaces of the SnBiAgIn solder and the SnBi solder is not very obvious (see Fig. 8f), because the fracture mechanism was not basically changed as the alloy elements have little influence on the Bi-rich phase. Also, the cleavage fracture should be more likely to occur at a high

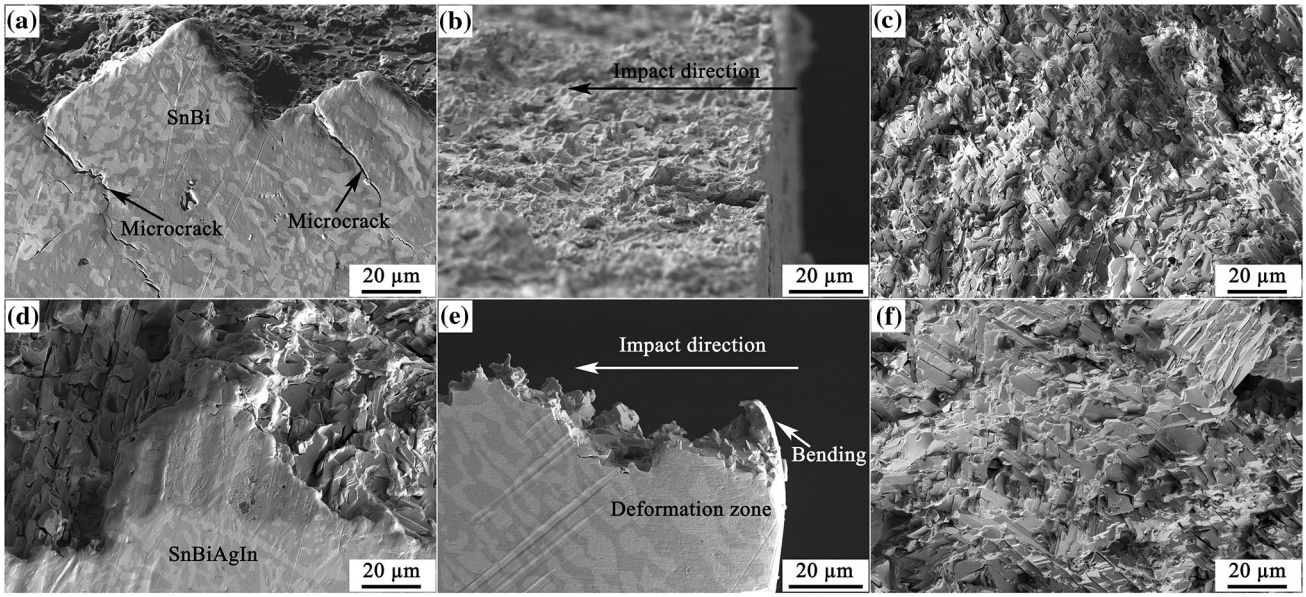

Fig. 8. Morphologies of the impact fracture surfaces: (a, b) side surfaces, and (c) fracture surfaces of the SnBi solder, (d, e) side surfaces, and (f) fracture surfaces of the SnBiAgIn solder.

strain rate during the impact process. Even so, it can be predicated from the deformation and fracture morphologies that the SnBiAgIn solder is more ductile than the SnBi eutectic solder under impact loading.

Influences of Ag and In on Sn-58Bi Eutectic Solder

It is easy to understand that the addition of Ag and In can increase the nanohardness of the Sn-rich phase and the microhardness of the solder due to solution strength. As the solid solubility of In in the Sn-rich phase is relatively high, the nanohardness of the Sn-rich phase and the microhardness of the solder increases after In addition. Also, it has been reported that the addition of the In element can improve the ductility of SnBi solder.[19] In contrast, the Ag_3Sn generated by adding 2.0% Ag element has a certain pinning effect on the dislocation movement,[20] so that the strength and the microhardness of the SnBiAg solder increases, whereas, the solid solubility of Ag in the Sn-rich phase is much lower, and most of the Ag element forms Ag_3Sn particles with Sn, making the nanohardness of the Sn-rich phase in the SnBiAg solder increase only a little with individual Ag addition. With the combined addition of the In and Ag elements, the strengthening and toughening effects of the In and the strengthening effects of the Ag occur at the same time. As a result, the SnBiAgIn alloy shows the highest impact toughness. The solid solution, strengthening and coarsening mechanisms of the Ag and In elements in the Sn-rich phases still need further exploration.

From the above results and discussion, it can be concluded that the microhardness and toughness of the SnBi solder were improved by adding a certain amount of Ag and In. The mechanical properties of the SnBiAgIn solder may be further optimized by adjusting the content of Ag and In in the solder. According to some early reports, a series of alloy elements are effective in the refinement of the SnBi solder.[23,26,27] If the coarsening of the SnBi(AgIn) solders in this study can be restrained or even that the solders can be refined, it can be expected that the ductility, microhardness and impact toughness of the solders can be further improved. Therefore, further alloying of SnBiAgIn solder with grain refinement elements should be beneficial for its ductility and toughness.

CONCLUSIONS

In the current study, the influences of Ag and In on the microstructure, microhardness, and toughness of SnBi(AgIn) series solders were studied. Based on the results and discussion, it can be concluded that:

1. With 2.0 wt.% of Ag and 1.5 wt.% of In addition, the microstructure of SnBi solder shows different degrees of coarsening, especially for SnBiIn solder. Fine Ag_3Sn particles are formed in the Ag-containing solder, while large Ag_3Sn plates do not appear. The In-rich phases in the SnBiIn and SnBiAgIn solders are small.
2. The microhardness of the alloyed solders and the nanohardness of the Sn-rich phases in the alloyed solders obviously increase compared with the SnBi solder, which is mainly due to

the solution strengthening of In and the precipitation strengthening of the Ag_3Sn IMC. The nanohardness of the Bi-rich phases change little after alloying.

3. The impact toughness of the SnBiAgIn solder is obviously higher compared with the SnBi eutectic solder, because the plastic deformation is increased in the SnBiAgIn solder as In alloying can improve the ductility, and both the Ag and In addition can improve the strength of the Sn-rich phase in the solder.

ACKNOWLEDGMENTS

The authors would like to acknowledge Y.R. Yao, C.T. Wang and R.R. Jiang for microstructure observation, nano indentation and microhardness tests. This work was financially supported by the Natural Science Foundation of Zhejiang Province under Grant No. LQ20E050005, the National Natural Science Foundation of China under Grant No. 52001317.

CONFLICT OF INTEREST

The authors declare that they have no conflict of interest.

REFERENCES

1. S.N. Esfahani, S. Asghari, and S. Rashid-Nadimi, *Sol. Energy* 148, 49 (2017).
2. U.R. Kattner, *JOM* 54, 45 (2002).
3. S.F. Cheng, C.M. Huang, and M. Pecht, *Microelectron. Reliab.* 75, 77 (2017).
4. S. Sahasrabudhe, S. Mokler, M. Renavikar, S. Sane, K. Byrd, E. Brigham, O. Jin, P. Goonetilleke, N. Badwe, and S. Parupalli, in *2018 IEEE 68th Electronic Components and Technology Conference* (2018), pp. 1455–1464.
5. S. Mokler, R. Aspandiar, K. Byrd, O. Chen, S. Walwadkar, K.K. Tang, M. Renavikar, and S. Sane, in *Proceedings of SMTA International* (2016), pp. 318–326.
6. M.T. Zarmai, N.N. Ekere, C.F. Oduoza, and E.H. Amalu, *Appl. Energy* 154, 173 (2015).
7. F.J. Wang, H. Chen, Y. Huang, L.T. Liu, and Z.J. Zhang, *J. Mater. Sci.: Mater. Electron.* 30, 3222 (2019).
8. Q.K. Zhang, H.F. Zou, and Z.F. Zhang, *J. Mater. Res.* 25, 303 (2010).
9. M. McCormack, H.S. Chen, G.W. Kammlott, and S. Jin, *J. Electron. Mater.* 26, 954 (1997).
10. P.L. Liu and J.K. Shang, *J. Mater. Res.* 16, 1651 (2001).
11. H.F. Zou, Q.K. Zhang, and Z.F. Zhang, *Scr. Mater.* 61, 308 (2009).
12. G. Ren, I.J. Wilding, and M.N. Collins, *J. Alloys Compd.* 665, 251 (2016).
13. L. Zhang, L. Sun, and Y.H. Guo, *J. Mater. Sci.: Mater. Electron.* 26, 7629 (2015).
14. P. Šebo, P. Švec Sr, D. Janičkovič, E. Illeková, M. Zemánková, Y. Plevachuk, and V. Sidorov, *Mater. Sci. Eng., A* 571, 184 (2013).
15. F.Q. Hu, Q.K. Zhang, J.J. Jiang, and Z.L. Song, *Mater. Lett.* 214, 142 (2018).
16. L.Z. Yang, W. Zhou, Y. Ma, X.Z. Li, Y.H. Liang, W.Q. Cui, and P. Wu, *Mater. Sci. Eng., A* 667, 368 (2016).
17. S.K. Lin, T.L. Nguyen, S.C. Wu, and Y.H. Wang, *J. Alloys Compd.* 586, 319 (2014).
18. J. Shen, Y.Y. Pu, H.G. Yin, D.J. Luo, and J. Chen, *J. Alloys Compd.* 614, 63 (2014).
19. O. Mokhtari and H. Nishikawa, *Mater. Sci. Eng., A* 651, 831 (2016).
20. X. Chen, F. Xue, J. Zhou, and Y. Yao, *J. Alloys Compd.* 633, 377 (2015).
21. Z. Wang, Q.K. Zhang, Y.X. Chen, and Z.L. Song, *J. Mater. Sci.: Mater. Electron.* 30, 18524 (2019).
22. R.M. Shalaby, *Mater. Sci. Eng., A* 560, 86 (2013).
23. J. Shen, C.P. Wu, and S.Z. Li, *J. Mater. Sci.: Mater. Electron.* 23, 156 (2012).
24. B.L. Silva, A. Garcia, and J.E. Spinelli, *Mater. Charact.* 114, 30 (2016).
25. Y.M. Liu and T.H. Chuang, *J. Electron. Mater.* 29, 1328 (2000).
26. W.B. Zhu, W.W. Zhang, W. Zhou, and P. Wu, *J. Alloys Compd.* 789, 805 (2019).
27. Y. Li, K.M. Luo, A.B.Y. Lim, Z. Chen, F.S. Wu, and Y.C. Chan, *Mater. Sci. Eng., A* 669, 291 (2016).